Glu-Ureido–Based Inhibitors of Prostate-Specific Membrane Antigen: Lessons Learned During the Development of a Novel Class of Low-Molecular-Weight Theranostic Radiotracers

Klaus Kopka[1,2], Martina Benešová[3,4], Cyril Bařinka[5], Uwe Haberkorn[6,7], and John Babich[8]

[1]Division of Radiopharmaceutical Chemistry, German Cancer Research Center, INF 280, Heidelberg, Germany; [2]German Cancer Consortium (DKTK), Heidelberg, Germany; [3]Department of Chemistry and Applied Biosciences, ETH Zurich, Zurich, Switzerland; [4]Center for Radiopharmaceutical Sciences ETH-PSI-USZ, Paul Scherrer Institut, Villigen, Switzerland; [5]Laboratory of Structural Biology, Institute of Biotechnology CAS, Prumyslova, Vestec, Czech Republic; [6]Department of Nuclear Medicine, University of Heidelberg, INF 400, Heidelberg, Germany; [7]Clinical Cooperation Unit Nuclear Medicine, German Cancer Research Center, INF 280, Heidelberg, Germany; and [8]Division of Radiopharmaceutical Sciences and Molecular Imaging Innovations Institute, Department of Radiology, Weill Cornell Medicine, New York, New York

In recent years, several radioligands targeting prostate-specific membrane antigen (PSMA) have been clinically introduced as a new class of theranostic radiopharmaceuticals for the treatment of prostate cancer (PC). In the second decade of the 21st century, a new era in nuclear medicine was initiated by the clinical introduction of small-molecule PSMA inhibitor radioligands, 40 y after the clinical introduction of ^{18}F-FDG. Because of the high incidence and mortality of PC, the new PSMA radioligands have already had a remarkable impact on the clinical management of PC. For the continuing clinical development and long-term success of theranostic agents, designing modern prospective clinical trials in theranostic nuclear medicine is essential. First-in-human studies with PSMA radioligands derived from small-molecule PSMA inhibitors showed highly sensitive imaging of PSMA-positive PC by means of PET and SPECT as well as a dramatic response of metastatic castration-resistant PC after PSMA radioligand therapy. This tremendous success logically led to the initiation of prospective clinical trials with several PSMA radioligands. Meanwhile, MIP-1404, PSMA-11, 2-(3-{1-carboxy-5-[(6-fluoro-pyridine-3-carbonyl)-amino]-pentyl}-ureido)-pentanedioic acid (DCFPyL), PSMA-617, PSMA-1007, and others have entered or will enter prospective clinical trials soon in several countries. The significance becomes apparent by, for example, the considerable increase in the number of publications about PSMA-targeted PET imaging from 2013 to 2016 (e.g., a search of the Web of Science for "PSMA" AND "PET" found only 19 publications in 2013 but 218 in 2016). Closer examination of the initial success of PC treatment with PSMA inhibitor radiotracers leads to several questions from the basic research perspective as well as from the perspective of clinical demands: What lessons have been learned regarding the design of PSMA radioligands that have already been developed? Has an acceptable compromise between optimal PSMA radioligand design and a broad range of clinical demands been reached? Can the lessons learned from multiple successes within the PSMA experience be transferred to further theranostic approaches?

Received Feb. 16, 2017; revision accepted Mar. 27, 2017.

For correspondence or reprints contact: Klaus Kopka, Division of Radiopharmaceutical Chemistry, German Cancer Research Center, INF 280, 69120 Heidelberg, Germany.

E-mail: k.kopka@dkfz.de

Key Words: small-molecule PSMA inhibitors; theranostic PSMA radioligands; PSMA radiotracers; prostate cancer; radioligand therapy

J Nucl Med 2017; 58:17S–26S

DOI: 10.2967/jnumed.116.186775

PROLOG

A new era in nuclear medicine was initiated during the 21st century by the clinical introduction of a new class of small-molecule prostate-specific membrane antigen (PSMA) inhibitor radiotracers, just 40 y after the clinical introduction of ^{18}F-FDG. PSMA radioligands are of utmost clinical interest and show promise for the diagnosis and therapy of prostate cancer (PC). However, what lessons have been learned regarding the design of PSMA radioligands that have already been developed? Has an acceptable compromise between optimal PSMA radioligand design and compliance with clinical demands been found? Can the PSMA radioligand approach be transferred to the development of other targeted theranostic approaches? These key questions are addressed in 4 lessons from the basic research and clinical demand perspectives: lesson 1, retrospective on Glu-ureido–based PSMA radioligands of clinical relevance; lesson 2, need for structure-aided design of Glu-ureido–based PSMA radioligands; lesson 3, elucidation of structure–property relationships with in vitro, in vivo, and ex vivo assays; and lesson 4, consideration of how to transfer the PSMA radioligand approach to other targeted theranostic approaches (e.g., tumor heterogeneity).

LESSON 1: RETROSPECTIVE ON GLU-UREIDO–BASED PSMA RADIOLIGANDS OF CLINICAL RELEVANCE

Recent literature contains comprehensive reviews that summarize the substance class of small-molecule and low-molecular-weight peptidomimetic Glu-ureido–based PSMA inhibitors. A few recently published reviews provide a comprehensive overview of the current status of small-molecule PSMA inhibitor radiotracers (*1–4*).

Several PSMA radioligands have already entered clinical settings and are being used for the diagnosis and radioligand therapy (RLT) of PC. The first small-molecule inhibitors of PSMA

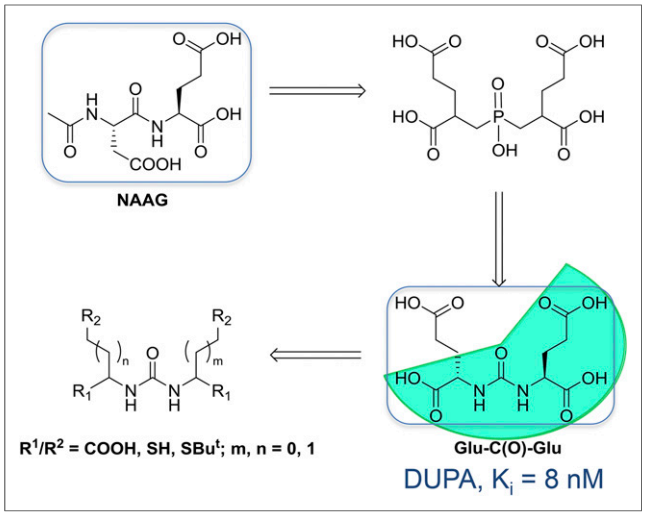

FIGURE 1. Glu-ureido–based PSMA inhibitor exemplifying rational design of urea-based glutamate carboxypeptidase II inhibitors. DUPA = 2-[3-(1,3-dicarboxypropyl)ureido]pentanedioic acid; NAAG = *N*-acetyl-L-aspartyl-L-glutamate. (Reprinted with permission of (*9*).)

for the imaging of PC were introduced into clinical settings in 2008 by Molecular Insight Pharmaceuticals, Inc. (MIP, now a subsidiary of Progenics Pharmaceuticals Inc.) (ClinicalTrials.gov identifier: NCT00712829). These ligands, ^{123}I-MIP-1072 and ^{123}I-MIP-1095, were based on the Glu-urea-Lys motif and contained aromatic substituents for stable introduction of the single-photon-emitting radionuclide ^{123}I (half-life, 13.2 h) (*5,6*). However, worldwide, ^{68}Ga-PSMA-11 currently is the most prominent ^{68}Ga-labeled PSMA radioligand for the PET imaging of PSMA-positive PC. ^{68}Ga-PSMA-11 was clinically introduced several years ago (*7,8*). PSMA-11 belongs to the class of low-molecular-weight Glu-ureido–based PSMA inhibitors. In general, the class of urea-based PSMA inhibitors was first described by Kozikowski et al. (*9,10*), building on the work of Jackson et al. (*11,12*), and introduced as a peptidomimetic counterpart of the most abundant peptidyl neurotransmitter, *N*-acetyl-L-aspartyl-L-glutamate (Fig. 1). One of the first preclinical imaging studies with small-molecule PSMA inhibitor radioligands in PSMA-positive tumor xenografts was reported by Foss et al. in 2005 (Fig. 2) (*13*).

In principle, small-molecule PSMA inhibitors bind to PSMA, also called glutamate carboxypeptidase II or *N*-acetylated α-linked acidic dipeptidase/*N*-acetyl-L-aspartyl-L-glutamate peptidase I, which is a binuclear membrane-bound zinc protease (MEROPS [peptidase database; http://merops.sanger.ac.uk/] identifier: M28.010) that is highly upregulated in all stages of PC with nearly no expression in healthy tissues. Moreover, there is a significant correlation between the level of expression of PSMA and the progression of the disease (*14–16*). PSMA is thus an optimal target for both the imaging and the endoradiotherapy of PC.

The preclinical evaluation of ^{68}Ga-PSMA-11 (also called ^{68}Ga-DKFZ-PSMA-11 or ^{68}Ga-PSMA-HBED-CC) (*17*) encouraged the aforementioned clinical introduction of this promising PC imaging agent in Heidelberg, Germany. The complexing agent *N*,*N*´-bis[2-hydroxy-5-(carboxyethyl)benzyl]-ethylenediamine-*N*,*N*´-diacetic acid (HBED-CC) was conjugated to the pharmacophore Glu-urea-Lys via the aminohexanoic acid linker. The resulting conjugate, PSMA–HBED-CC (PSMA-11), could not bind to clinically relevant therapeutic radiometals, such as ^{177}Lu or ^{225}Ac. Therefore, PSMA-11 could be used only for diagnostic purposes. However, it soon became clear that PSMA inhibitors could also be used for PSMA RLT of PC. The first clinical theranostic approach with radioiodinated versions of PSMA inhibitor MIP-1095 for the treatment of patients with late-stage disease (that is, metastatic castration-resistant PC) was reported in 2014 (*18*). The tracer MIP-1095 was first described by Hillier et al. in 2009 (Fig. 3) (*5*), and the first-in-human evaluation of the ^{123}I-labeled version was finally published in 2013 (*19*).

As a consequence of those findings, the group in Heidelberg, Germany, started an initiative to transform the diagnostic tracer PSMA-11 into the theranostic variant PSMA-617, which can also be radiolabeled with the therapeutically relevant trivalent radiometals ^{177}Lu or ^{90}Y for β-therapy and ^{225}Ac for α-therapy. Of 18 DOTA conjugates with optimized linker moieties between the Glu-urea-Lys–binding motif and the DOTA chelator, PSMA-617 was identified as the best candidate for translation to clinical settings (*20,21*). In parallel, another theranostic PSMA radioligand, PSMA for imaging and therapy (PSMA I&T), was also described (*22,23*). ^{177}Lu-PSMA-617 and the ^{225}Ac-labeled version are currently the main candidates for endoradiotherapy (i.e., PSMA RLT) of PC (*24–27*).

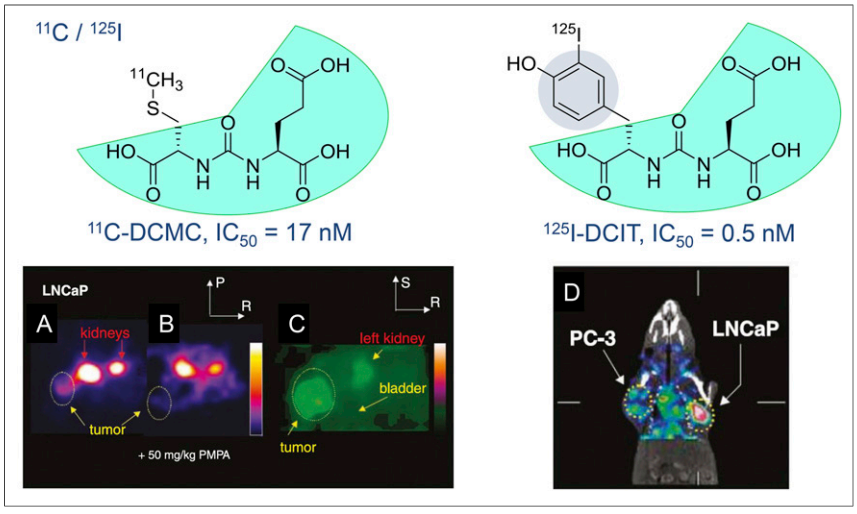

FIGURE 2. In vivo examinations of radiolabeled small-molecule PSMA inhibitors in experimental models of PC. (A and B) Axial PET images of *N*-[*N*-[(*S*)-1,3-dicarboxypropyl]carbamoyl]-*S*-^{11}C-methyl-L-cysteine (^{11}C-DCMC) in mouse kidney and LNCaP tumors without (A) and with (B) coinjection of 2-(phosphonomethyl)pentane-1,5-dioic acid (PMPA) at 50 mg/kg to block PSMA. (C) Magnified, coronal reconstructed image of animal in A outside plane of kidneys immediately after urination indicates lack of specific binding to bladder. Tumor and portion of left kidney were clearly visualized. Images in A and B were scaled to same maximum. IC_{50} = 50% inhibitory concentration; P = posterior, R = right, S = superior. (D) SPECT with CT overlay shows uptake of *N*-[*N*-[(*S*)-1,3-dicarboxypropyl]carbamoyl]-*S*-3-^{125}I-iodo-L-tyrosine (^{125}I-DCIT) in LNCaP tumor, whereas PC-3 tumor retains only minimal radiotracer. (Reprinted with permission of (*13*).)

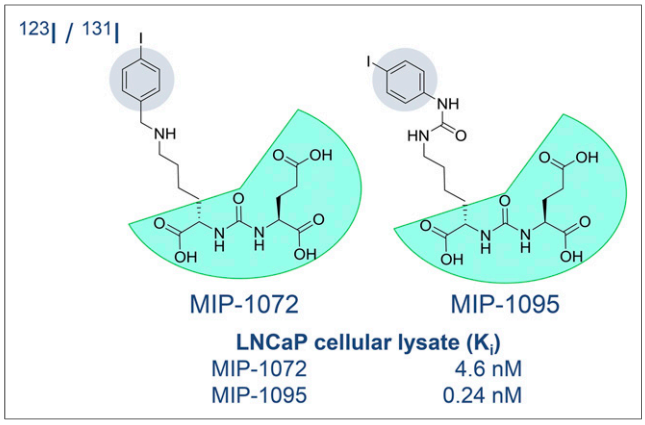

FIGURE 3. Radioiodinated ("haloaromatic") Glu-ureido–based PSMA inhibitors (MIP compounds)—MIP-1072: 2-(3-(1-carboxy-5-(4-iodo-benzylamino)pentyl)ureido)pentanedioic acid; MIP-1095: (*S*)-2-(3-((*R*)-1-carboxy-5-(3-(4-iodophenyl)ureido)pentyl)ureido)pentanedioic acid (*5,6,18,19*).

Because of large numbers of patients and the hitherto limited capacity for the production of the radiometal-based PET tracer ^{68}Ga-PSMA-11, there is also a need for ^{18}F-labeled PSMA ligands. With PSMA-617 as the lead structure, the PET tracer ^{18}F-PSMA-1007 was recently developed; this agent is an ideal and promising ^{18}F-labeled PSMA inhibitor for prostate PET imaging, especially for the primary diagnosis of PC (*28*). The clinical potential of this novel PSMA-targeted PET radioligand is currently being explored (*29,30*). The ^{18}F-labeled PET radioligands *N*-[*N*-[(*S*)-1,3-dicarboxypropyl]carbamoyl]-4-fluorobenzyl-L-cysteine (^{18}F-DCFBC) (*31–33*) and DCFPyL (^{18}F-DCFPyL) (*34,35*) were recently introduced into clinical settings as well. In contrast, ^{18}F-PSMA-1007 has the advantage that tracer-associated activity accumulation in the urinary bladder over time is almost not observable; this advantage makes this ^{18}F-labeled PSMA radioligand an ideal candidate for the primary diagnosis of PC and the staging of local recurrent disease (*29,30*).

Figure 4 shows all of the Glu-ureido–based PSMA radioligands that we consider to be clinically relevant for both SPECT and PET diagnostics and PSMA RLT.

The promising SPECT PSMA radioligands MIP-1404 (*36,37*) and PSMA for imaging and surgery (PSMA I&S) (*38*) are also in clinical development, with MIP-1404 being the first PSMA imaging agent to finalize phase 3 clinical trials. Uniquely, the iodine-containing MIP-1095 can be used for SPECT (the ^{123}I-labeled version), for PET (the ^{124}I-labeled version), and for RLT (the ^{131}I-labeled version and possibly the ^{211}At version for α-therapy). ^{68}Ga-PSMA-11, ^{18}F-DCFBC, ^{18}F-DCFPyL, and ^{18}F-PSMA-1007 are exclusive PET PSMA radioligands. PSMA-617 and PSMA I&T are theranostic PSMA radioligands because they can be radiolabeled with both diagnostic (e.g., ^{68}Ga and ^{44}Sc) and therapeutic (e.g., ^{177}Lu) radiometals (*23,39,40*). Because PSMA-1007 is derived from PSMA-617, the tracers (^{18}F-PSMA-1007 and ^{177}Lu-PSMA-617) can be used as a theranostic

Cpd.	MIP-1095	DCFBC	DCFPyL	MIP-1404, Trofolastat	PSMA I&T
Chemical Structure	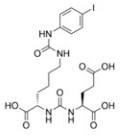	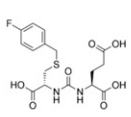	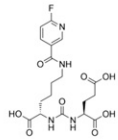	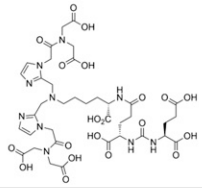	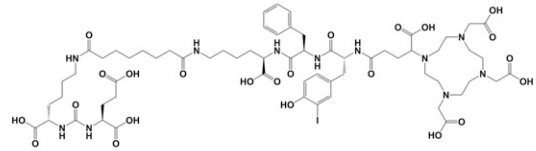
Class	Theranostic	Diagnostic PET	Diagnostic PET	Diagnostic SPECT	Theranostic
RN	^{123}I ^{124}I ^{131}I	^{18}F	^{18}F	^{99m}Tc	^{68}Ga ^{177}Lu ^{111}In
Ref.	(5,6,18, 19)	(31-33)	(34, 35)	(36, 37)	(22, 23)

Cpd.	PSMA-617	PSMA-11	PSMA-1007	PSMA I&S
Chemical Structure	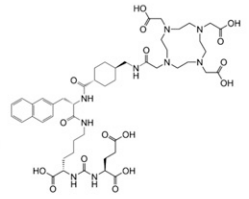	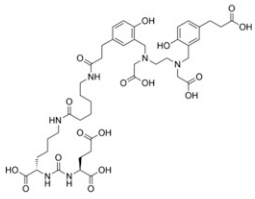	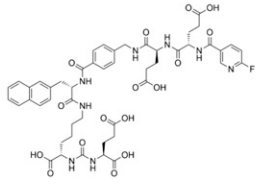	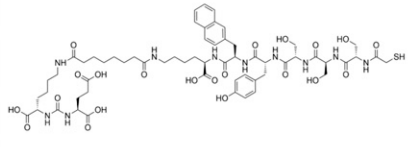
Class	Theranostic	Diagnostic PET	Diagnostic PET	Diagnostic SPECT
RN	^{68}Ga ^{177}Lu ^{225}Ac	^{68}Ga	^{18}F	^{99m}Tc
Ref.	(20, 21, 24-27)	(7,8,17)	(28-30)	(38)

FIGURE 4. Glu-ureido–based PSMA radioligands of clinical relevance. Cpd. = compound; Ref. = reference; RN = radionuclide.

tandem of PSMA radioligands. Other tandem combinations are also possible because the diagnostic component need not be an exact replica of the therapeutic component.

What Have We Learned from Lesson 1? Taking into account the data about the Glu-ureido–based PSMA radioligands that have already been clinically introduced (Fig. 4), we conclude that a good compromise between optimal PSMA radioligand design and compliance with clinical demands has been found. This conclusion is supported by the fact that prospective clinical trials are ongoing. For example, there are trials with ^{68}Ga-PSMA-11 (e.g., European Union Trials Register EudraCT 2016-001815-19 [German Cancer Consortium trial]; ClinicalTrials.gov NCT02919111 [PSMA PreRP]), ^{18}F-DCFPyL (e.g., ClinicalTrials.gov NCT02981368 [OSPREY]), ^{131}I-MIP-1095 (e.g., ClinicalTrials.gov NCT03030885), ^{99m}Tc-MIP-1404 (e.g., European Union Trials Register EudraCT 2012-001864-30; ClinicalTrials.gov NCT02615067 [proSPECT-AS]), and ^{177}Lu-PSMA-617 (e.g., ClinicalTrials.gov NCT03042468). It is expected that ^{99m}Tc-MIP-1404 (Trofolastat) will be launched on the market as the first low-molecular-weight SPECT PSMA radioligand because a phase 3 clinical trial with this tracer is already under way. The structure-aided characterization (lesson 2) and the elucidation of the structure–property relationships of the Glu-ureido–based PSMA inhibitors (lesson 3) may help in deciding whether the design of PSMA radioligands that have already been developed is optimal for PC imaging and endoradiotherapy (see the PSMA-binding motif of the PSMA radioligands, shaded in cyan in Figs. 1–3).

LESSON 2: NEED FOR STRUCTURE-AIDED DESIGN OF GLU-UREIDO–BASED PSMA RADIOLIGANDS

Structural studies of PSMA–ligand complexes provided mechanistic insight into interactions governing ligand recognition by the enzyme. They helped in rationalizing a vast amount of available structure–activity relationship data and were later used for the structure-aided design of the next generation of PSMA ligands. The first PSMA crystal structures were reported more than a decade ago (*41,42*), and now more than 60 x-ray crystallographic structures of PSMA–ligand complexes are publicly available at the Protein Data Bank (PDB) (www.rcsb.org).

The PSMA internal inhibitor–binding cavity can be roughly divided into 3 continuous parts: the S1′ glutamate recognition pocket, the dinuclear zinc(II) active site, and an irregularly shaped entrance funnel connecting the active site to the external surface of PSMA (Fig. 5) (*43*). This structural arrangement is reflected in turn in the inhibitor design, for which all currently used Glu-ureido–based PSMA ligands comprise a terminal glutamate moiety connected to a linker/effector part via the zinc-binding ureido functionality. Such ligands therefore can be viewed as a composite of 3 semi-independent modules that can be tailored to suit experimental or clinical needs.

Originally, efforts regarding extensive structure–activity relationships were aimed at identifying permissible substitutions of the terminal glutamate that would improve the physicochemical and biologic characteristics of target ligands. However, all such substitutions reported to date have failed to provide viable leads and instead have resulted in compounds with substantially lower PSMA affinities (*9,44–46*). Likewise, a search for a new "ultimate" zinc-binding group has not been successful; consequently, ureido-based PSMA inhibitor scaffolds are currently the most prevalent theranostic PSMA-targeting vectors used, followed only by transition-state mimetics, such as phosphoramidates (*47*).

In recent years, researchers turned their attention to modifications at the linker/functional spacer/effector portion of Glu-ureido–based ligands, and this approach resulted in several clinically validated compounds, such as PSMA-617 (*20,21*). Such modifications are well tolerated by PSMA because of the fact that, unlike the constricted S1′ glutamate recognition pocket, the entrance funnel is quite spacious and can accommodate many diverse chemical groups (*43,48–50*). Typically, a flexible aminohexanoyl moiety is used as the proximal segment of the linker. The P1 carboxylate group, which is the common denominator of many, but not all, Glu-ureido–based ligands, is critical for high-affinity PSMA binding and therefore can be viewed as an integral part of the Glu-ureido pharmacophore (*45*). The flexibility of the proximal linker enables "optimal" positioning of coupled functional spacers or effector moieties within the amphipathic entrance funnel. Additionally, it facilitates the engagement of these moieties with structurally defined pockets in the entrance funnel (e.g., the S1 accessory hydrophobic pocket or the arene-binding site), thus contributing to the increased affinity of such bivalent ligands for PSMA (Fig. 6) and allowing for the structure-assisted design of the next generation of ligands (*48,51–55*).

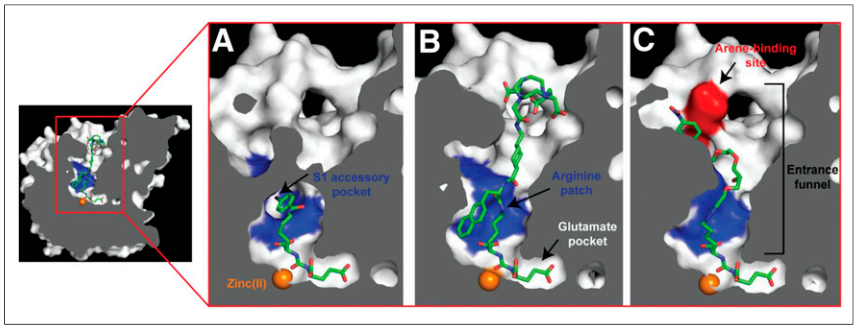

FIGURE 5. Internal cavity of PSMA. Cross-section of PSMA showing internal inhibitor-binding cavity comprising S1′ glutamate recognition pocket, dinuclear zinc(II) active site, and irregularly shaped entrance funnel. Although S1′ glutamate recognition pocket is restricted in size and shape, spacious entrance funnel can accommodate functional groups of different sizes and physicochemical characteristics. Within entrance funnel, arginine patch, S1 accessory hydrophobic pocket, and arene-binding site—prominent structural features used for inhibitor design—are highlighted. Zinc ions are shown as orange spheres, and PSMA ligands are shown as stick representations: DCIBzL (A) (PDB code 3D7H), PSMA-617 (B) (unpublished data), and ARM-P4 (C) (PDB code 2XEG).

What Have We Learned from Lesson 2? It is obvious that the proximal linker/functional spacer will be a hot spot for modifications aimed at the development of new Glu-ureido–based PSMA ligands. It is hoped that the designed ligands, aided by x-ray crystallography, will tap into structural features of the entrance funnel that have not been thoroughly explored, resulting in their improved inhibitory or biologic characteristics. Additionally, such modifications may help in creating ligands that could be truly PSMA specific by selectively tar-

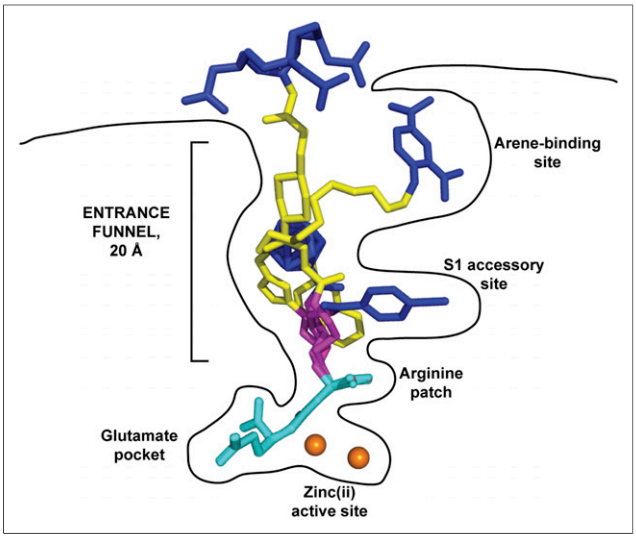

FIGURE 6. Glu-ureido–based ligands within binding cavity of PSMA. Complexes between PSMA and 4 Glu-ureido–based ligands are superimposed on corresponding Cα atoms of protein. Although there is complete structural overlap of pharmacophore modules (cyan), positioning of flexible proximal linker (magenta), functional spacer (yellow), and effector moiety (blue) is divergent within (and outside) amphipathic entrance funnel. Zinc ions are shown as orange spheres. PSMA–inhibitor complexes used were DCIBzL (PDB code 3D7H) (*48*), ARM-P4 (PDB code 2XEG) (*52*), carborane (PDB code 4OME) (*55*), and PSMA-617 (unpublished data).

geting PSMA (i.e., glutamate carboxypeptidase II)—a property that would be advantageous for therapeutic applications. Finally, on the basis of the structural characterization of PSMA–ligand complexes so far, in some cases, the functional spacer or effector moiety contributes substantially to the PSMA affinity of a given ligand and therefore can be viewed as an extension of the original Glu-urea-Lys pharmacophore motif—in other words, an affinity enhancer.

LESSON 3: ELUCIDATING STRUCTURE–PROPERTY RELATIONSHIPS WITH IN VITRO, IN VIVO, AND EX VIVO ASSAYS

The applicability of highly potent PSMA inhibitors can be predicted through systematic preclinical in vitro, in vivo, and ex vivo evaluations.

In vitro experiments with newly designed PSMA inhibitors are usually performed using the PSMA-positive lymph node carcinoma of the prostate (LNCaP) cell line, derived from an androgen-sensitive human lymph node metastatic lesion of prostatic adenocarcinoma (*56*) or, more recently, using the transfected human PSMA–expressing PC-3 PIP cell line (PC-3 transfected to stably express the human PSMA protein) and the human PSMA–deficient PC-3 flu cell line (*39*). The main focus is examination of the PSMA-binding affinity and the cellular internalization behavior. Moreover, in vivo imaging of tumor-bearing mice or rats reveals variable tumor visualization as well as clearance of radiolabeled compounds from the kidneys and the whole body. Finally, ex vivo biodistribution demonstrating radioactivity accumulation in tumors, all relevant organs (e.g., salivary glands, spleen, liver, kidneys, and intestines), the blood, and muscles provides the clearest evidence for selection of the most promising compounds.

It is not surprising that significant structure-dependent differences between individual PSMA inhibitors are generally observed. In the development of PSMA-617, PSMA inhibition potency, cellular internalization, and imaging quality could be strongly influenced even by slight differences in the linker moiety between the PSMA-targeting Glu-urea-Lys–binding motif and the DOTA chelator (*20*). In that study, the in vitro results, especially internalization of the ligand by LNCaP cells, correlated highly with the in vivo tumor imaging properties. Thus, cellular internalization in vitro seems to be necessary for in vivo success, especially for endoradiotherapy (i.e., PSMA RLT). Moreover, it was shown that introducing a hydrophobic group(s) might interfere with PSMA-binding ability because lipophilicity influenced the clearance of radioactivity by the kidneys and from the background (*20*).

Another example involves the widely used diagnostic radiotracer ^{68}Ga-PSMA-11 (*8*), which served (among others) as the benchmark for the development of a DOTA-conjugated theranostic counterpart (Fig. 7). Eder et al. reported that direct replacement of the HBED-CC chelator in PSMA-11 by the DOTA chelator resulted in significant diminution of the tumor-targeting properties of the new compound (*17*). Thus, the original aminohexanoic acid linker in PSMA-11 was redesigned to mimic the proven biologic interactions of HBED-CC with the PSMA-binding pocket(s). An extensive preclinical evaluation provided an effective strategy for producing highly potent DOTA-conjugated PSMA inhibitors attaining sufficient PSMA-dependent cellular internalization, akin to that of PSMA-11, and improving the pharmacokinetic properties. The optimal properties were finally attributed to PSMA-617 (*20,21*).

A side-by-side in vitro comparison of PSMA-617 and PSMA-11 is shown in Table 1. The PSMA inhibition potency and internalization into LNCaP cells were greater for PSMA-617. The diverse behavior of these 2 inhibitors was also demonstrated by dynamic

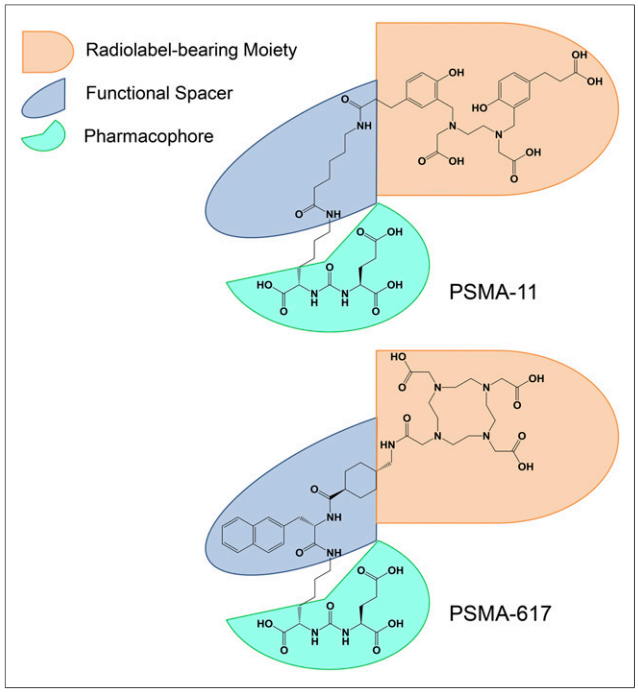

FIGURE 7. Dependence of transformation of diagnostic tracer PSMA-11 into theranostic variant PSMA-617 on structural arrangement of pharmacophore, functional spacer, and radiolabel-bearing/effector moiety.

TABLE 1
PSMA Inhibition Potency (K_i) and Cellular Internalization of PSMA-11 and PSMA-617, as Determined with LNCaP Cells (*21*)

Compound	K_i (nM)	Internalization
^{68}Ga-PSMA-11	12.0 ± 2.8	9.47 ± 2.56
^{68}Ga-PSMA-617	2.34 ± 2.94	17.67 ± 4.34

Data are reported as mean ± SD. Internalization is reported as percentage applied activity/10^6 LNCaP cells.

small-animal PET imaging (Fig. 8) and ex vivo organ distribution (Fig. 9). Major differences were observed in the spleen (17.88 ± 2.87 [mean ± SD] percentage injected dose/g [%ID/g] for PSMA-11 and 2.13 ± 0.16 %ID/g for PSMA-617) at 1 h after injection and in the kidneys (187.4 ± 25.3 %ID/g for PSMA-11 and 2.13 ± 1.36 %ID/g for PSMA-617) and the tumor (3.20 ± 2.89 %ID/g for PSMA-11 and 10.58 ± 4.50 %ID/g for PSMA-617) at 24 h after injection. Compared with the results at 1 h after injection, the kidney uptake of PSMA-11 was not significantly reduced at 24 h after injection, whereas PSMA-617 was nearly completely cleared. Such rapid renal clearance of radioactivity is necessary to reduce potential radiation toxicity (radiotoxicity) to the kidneys and to avoid possible chronic long-term side effects of PSMA-specific endoradiotherapy (*21*).

Taken together, data from systematic in vitro, in vivo, and ex vivo preclinical evaluations are important for elucidating the structure–property relationships of prospective PSMA inhibitors and for clarifying the effects of structural modifications on the tumor-targeting and pharmacokinetic properties. This strategy might lead to more accurate rational and structure-aided design of new urea-based PSMA-targeted and other radioligands.

What Have We Learned from Lesson 3? A careful preclinical evaluation of structure–property relationships connects the molecular structure of PSMA ligands with in vitro (e.g., inhibition constants [50% inhibitory concentration and K_i] and dissociation constant [K_d]), ex vivo (e.g., %ID/g), and in vivo (e.g., SUV) data. Further in vitro data, such as lipophilicity, and the optimal specific/molar activity of the radioligand used for imaging and therapy, should also be considered in relationship to PSMA inhibition potency. For transformation of the exclusive diagnostic PET tracer PSMA-11 into a theranostic version (in this case, PSMA-617), elucidation of the structure–property relationships was the main prerequisite for identifying the optimal candidate (PSMA-617). PSMA-617 can now be labeled with both therapeutic radionuclides (e.g., ^{90}Y, ^{177}Lu, and ^{225}Ac), having physical half-lives of several days, and short-lived diagnostic radionuclides (e.g., ^{68}Ga and ^{44}Sc).

The data suggest that rational design initiatives for a new series of PSMA radioligands should include careful examination of their structure–property relationships to reveal which variant is optimal for diagnostic or therapeutic applications or which variant is ideal for both imaging and therapy. Because even slight structural modifications of PSMA ligands can result in a complete loss or alteration of the necessary in vitro, ex vivo, and in vivo properties, a detailed preclinical characterization of a PSMA ligand is needed before clinical translation can be considered. Clinical demands (e.g., for primary diagnosis, diagnosis of relapse, or PSMA RLT of metastatic castration-resistant PC) require the best PSMA ligands for diagnostic or therapeutic PSMA-targeted PC treatment.

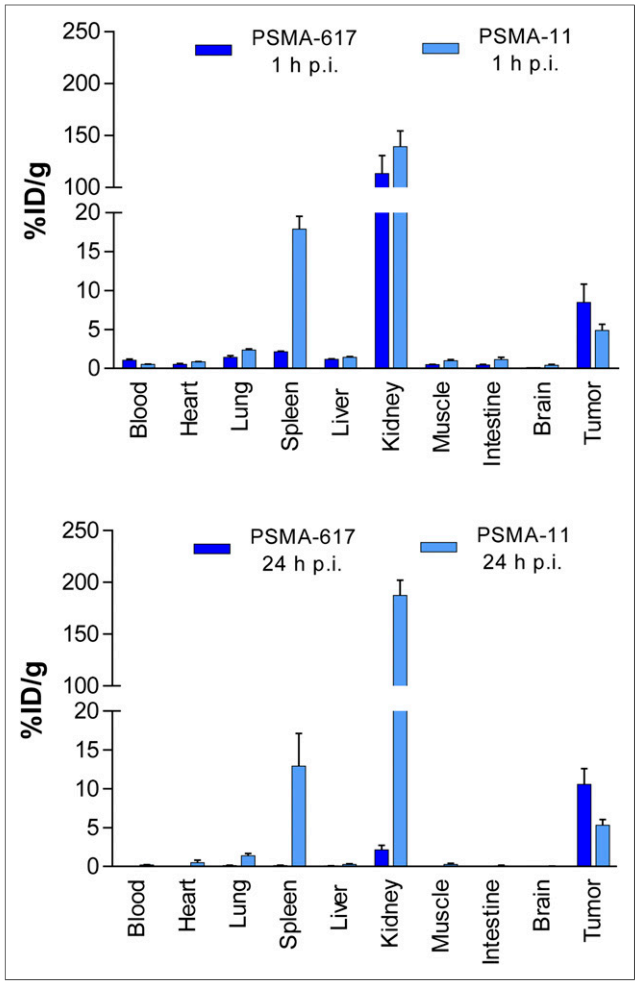

FIGURE 9. Organ distribution of ^{68}Ga-PSMA-617 and ^{68}Ga-PSMA-11 1 h after injection (p.i.) and of ^{177}Lu-PSMA-617 and ^{67}Ga-PSMA-11 24 h after injection. (Reprinted with permission of (*21*).)

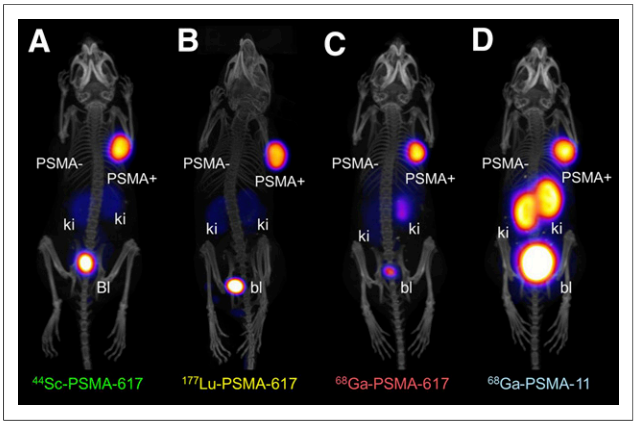

FIGURE 8. PET/CT and SPECT/CT imaging of PC-3 PIP/flu tumor-bearing mice. Tumor-targeting efficacy and pharmacokinetic properties were evaluated with ^{44}Sc-PSMA-617 (A), ^{177}Lu-PSMA-617 (B), ^{68}Ga-PSMA-617 (C), and ^{68}Ga-PSMA-11 (D) 2 h after injection. Bl or bl = bladder; ki = kidney. (Reprinted with permission of (*39*).)

LESSON 4: CONSIDERATION OF HOW TO TRANSFER PSMA RADIOLIGAND APPROACH TO OTHER TARGETED THERANOSTIC APPROACHES

For many years, several other classes of theranostic radioligand systems have been in preclinical and clinical development for imaging or peptide receptor radionuclide therapy (in addition to the prominent radioiodine therapy approach). These include, among others, radiolabeled peptide analogs, such as the somatostatin receptor (SSTR) (*57,58*), cholecystokinin 2 receptor (gastrin receptor) (*59,60*), gastrin-releasing peptide receptor (GRPr) (*61,62*), glucagon-like peptide 1 receptor (*63*), and C-X-C motif chemokine receptor 4 (CXCR4) (*64–66*) ligands. So far, the SSTR, GRPr, and CXCR4 radioligands have been the most promising in clinical settings.

In the state-of-the-art theranostic SSTR radioligand approach, clinically established radioligands are used for the treatment of refractory neuroendocrine tumors that predominantly upregulate subtype SSTR2, belonging to the G-protein–coupled receptor (GPCR) family (*57*). Since the 1980s, ^{111}In-diethylenetriaminepentaacetic acid-octreotide (OctreoScan; Mallinckrodt) has been used in clinical settings for neuroendocrine tumor imaging (*58*). With the introduction of commercially available ^{68}Ge/^{68}Ga generators, several PET tracers followed: ^{68}Ga-DOTATOC (U.S. Food and Drug Administration Orphan Drug Designation in 2014), ^{68}Ga-DOTATATE (U.S. Food and Drug Administration kit approval for NETSPOT [Advanced Accelerator Applications] in 2016), and ^{68}Ga-DOTANOC (*67–69*). The same DOTA conjugates have been used for peptide receptor radionuclide therapy (i.e., for SSTR2 radioligand therapy) when labeled with β-particle emitters (e.g., ^{90}Y and ^{177}Lu) or an α-particle emitter (e.g., ^{213}Bi) (*70,71*). For ^{177}Lu-DOTATATE (Lutathera; Advanced Accelerator Applications), expanded access has been granted for the "treatment of patients with inoperable, somatostatin receptor positive, midgut carcinoid tumors, progressive under somatostatin analog therapy" (ClinicalTrials.gov NCT02705313).

Theranostic SSTR antagonists, such as ^{68}Ga-DOTA-JR11 and ^{177}Lu-DOTA-JR11, have been propagated and suggested to have an advantage over SSTR agonists because SSTR antagonists are not readily internalized into tumor cells and therefore can label (putatively) more receptor sites in vivo (*72,73*). This is a unique and puzzling finding of utmost interest for this class of theranostic GPCR radioligands, and it can only be speculated that the described advantage of SSTR antagonists over SSTR agonists can be explained by factors such as the recognition of a larger number of binding sites by antagonists, slow dissociation of SSTR-bound antagonists, and delayed and slow internalization of antagonists (*74*).

PSMA does not belong to the GPCR family; it belongs to the membrane-type zinc peptidase family. For PSMA inhibitor radiotracers, there is evidence that the internalization of PSMA ligands into tumor cells must be improved to gain optimal uptake in tumor lesions over time—relevant especially for PSMA RLT (lesson 3) (*20,40*). Moreover, during preclinical evaluations of theranostic radioligands, the physiologic levels of expression of the target must be carefully considered; these levels should be orders of magnitude lower in the normal state than in the diseased state.

Importantly, only low levels of endogenous PSMA expression have been found in many organs (in addition to the normal prostate), including the proximal tubules of the kidneys, the lacrimal and salivary glands, the spleen, the intestinal brush border membranes, the liver, the testes, the ovaries, and the brain. These findings are among the main prerequisites for concluding that only low receptor levels are present in the normal state and that the chosen biologic target is highly upregulated in the diseased state—leading to the decision to start designing a new class of theranostic radioligands.

PSMA indeed is overexpressed in prostate cancer cells relative to normal prostate cells (>6-fold), the kidneys (>2,000-fold), and the intestines (>900-fold) (*75*). With 600,000–800,000 PSMA molecules per cancer cell (as determined on LNCaP cells), PSMA represents an important PC marker (*76*). Higher stages and higher grading of PC are associated with significant upregulation of PSMA; this association may imply a role of PSMA in the transformation and/or invasiveness of PC (*15,16,77*).

The fact that the physiologic function(s) of PSMA in the aforementioned tissues (other than the nervous and digestive systems) is mostly unknown should not hinder the initiation of efforts to design a new class of theranostic radioligands (*15,16,78–83*).

The design of an ideal agent for the imaging of a particular type of cancer must begin with the selection of a molecular target that is specific to the cancer in question and that is consistently expressed at high levels in tumor cells throughout the natural progression of the disease, preferably with no alteration in expression during therapy. The signal from tumor cells indicates the viable tumor mass and can be used to monitor disease burden. This information is particularly critical for assessing the presence of a tumor and changes in tumor mass and spread, for determining whether the disease is low-grade localized disease, and for determining the response to treatment in a patient with late-stage metastatic disease.

Ligand selection should be based on rapid uptake and persistent localization at the target site with minimal retention in nontarget tissue. Small molecules have a critical advantage over much larger constructs given their faster rate of clearance from the blood and increased tumor permeability, which allow them to evade physiologic barriers encountered by larger molecules, such as antibodies.

As detailed previously, PSMA was selected as the molecular target of choice because its expression is dramatically upregulated in poorly differentiated, metastatic, and hormone-refractory adenocarcinomas (*15*) as well as after androgen deprivation therapy (*84*) and in lymph node metastases (*85*).

The collective results to date therefore suggest that PSMA is an ideal target for the molecular imaging of PC. This notion has been repeatedly validated because several groups have successfully demonstrated that radiolabeled small-molecule inhibitors of PSMA have the potential to localize PC through common molecular imaging modalities, such as SPECT and PET. These novel PSMA-targeting tracers should affect clinical management by guiding appropriate patient-specific treatment strategies. It is likely that a sensitive and specific means of imaging PC and PC metastases would have a significant impact on the clinical management of PC by providing greater certainty about the presence and extent of disease during the course of a patient's life.

What Have We Learned from Lesson 4? Researchers have worked for decades on new classes of theranostic radioligands for the treatment of different tumor entities. Merging knowledge of the rational and structure-aided design of new small-molecule theranostic radioligands with understanding of the structure–property relationships of the ligands in vitro, ex vivo, and in vivo is necessary to find the optimal radiotracer for a particular biologic target to design the best treatment options for different types of cancer. Depending on the type of biologic target (the receptor) to be addressed (e.g., GPCR for SSTR and zinc protease for PSMA), any future class of theranostic radioligands must be designed to detect and treat a particular cancer, thereby addressing various clinical needs in oncology.

It is known that in some cases of PC, PSMA is not upregulated at all or is only heterogeneously upregulated in tumor and metastatic tissues (*86,87*). As an additional option, clinicians could consider other classes of theranostic radioligands, such as the GRPr radiotracers, to offer the best PC patient–centered care (*61*).

Diversity of biologic features in tumors indeed presents a problem not only for diagnosis but also for treatment, as shown by molecular analysis of multiple spatially separated samples obtained from primary renal carcinomas and associated metastatic sites. It was found that 63%–69% of all somatic mutations were not detectable across every tumor region. Furthermore, gene expression signatures for a good prognosis and a poor prognosis were detected in different regions of the same tumor (*88*). These findings mean that cancer cell clones with various phenotypes may exist in spatially separated regions within the same tumor and in different tumors within a single patient (*89*). The same is true for PC, in that genomic heterogeneity is observed within individual prostate glands and between patients (*90*). At the phenotype level, this finding has been demonstrated by immunohistochemistry for PSMA by Mannweiler et al. (*86*). In their analysis, PSMA-positive cells were often surrounded by areas that were negative for PSMA. In primary tumors as well as distant metastases, total or partial PSMA negativity and cytoplasmic positivity were seen, without a correlation with the Gleason score, histologic subtype, or localization of metastases. Therefore, novel strategies targeting 2 or more tumor-associated molecules may be needed to increase the efficacy of diagnosis and treatment of a cancer type.

A combined analysis at the RNA and protein levels for the expression of $\alpha_v\beta_3$-integrin, neurotensin receptor 1, PSMA, and prostate stem cell antigen (PSCA) was done in PC tumor cells and xenografts (*91*). Although there were discrepancies between increases at the RNA level and those at the protein level for $\alpha_v\beta_3$-integrin, neurotensin receptor 1, and PSCA, these proteins represent possible targets for the imaging and therapy of PC. Similar results were obtained in an immunohistochemistry study with antibodies against GRPr, PSCA, and PSMA (*92*). In lymph node metastases, GRPr positivity was seen in 85.7% of the cases; the corresponding results for PSCA and PSMA were 95.2% and 100%, respectively. In bone metastases, GRPr staining was positive in 52.9% of the cases; the corresponding results for PSCA and PSMA were 94.1% and 100%, respectively.

These data qualify PSCA and GRPr as alternative or better complementary targets for the diagnosis and therapy of PC.

EPILOG

In this article, we have attempted to address several issues related to the new class of small-molecule Glu-ureido–based PSMA inhibitor radiotracers from the basic research and clinical demand perspectives. We briefly discussed the diversity of biologic features in tumors (tumor heterogeneity), suggesting potential complementary biologic targets that could result in further theranostic radioligand approaches, at least for the treatment of PC (lesson 4).

First-in-human (phase 0 and 1) studies and prospective clinical trials in general are already under way to confirm the preclinical proof-of-concept validations for the human situation (lesson 1). First proof-of-concept studies with PSMA radioligands are highlighted in detail in Figure 2 of the article by Eiber et al. in this supplement issue of *The Journal of Nuclear Medicine*; side-by-side, only slight, but distinct, differences in the biodistribution behaviors of ^{68}Ga-PSMA-11, ^{68}Ga-PSMA I&T, ^{18}F-DCFBC, ^{18}F-DCFPyL, and ^{18}F-PSMA-1007 (Fig. 4) were seen in PC patients. This side-by-side comparison should be the next step in clinical settings. Phase 0 comparison studies were performed in the first human trials with PSMA inhibitors, namely, MIP-1072 and MIP-1095 (*19*), and in the initial clinical evaluation of MIP-1404 and MIP-1405 (*36*). Interindividual (or even intraindividual) patient examinations helped determine the optimal PSMA radioligand for each intended PC option (imaging or therapy). Tracer accumulation in normal organs, such as the salivary and lacrimal glands, the kidneys, the spleen, and the intestines (which is not directly comparable to the preclinical in vivo and ex vivo results [lesson 3]), must be assessed in patients as well, especially from the safety (radiation dosimetry) perspective. The outcome of such assessments (*18,26,29,40,93–97*) will show whether future generations of PSMA radioligands should still be considered for first-in-human studies or whether efforts targeting new complementary molecules should be undertaken to further increase the efficacy of the diagnosis and treatment of PC.

Transferring knowledge gained from the development of the new class of theranostic PSMA radioligands to further theranostic approaches in nuclear medicine is possible. This concept is underlined by the classes of theranostic radioligands (e.g., targeting SSTR, GRPr, and CXCR4) that have already been clinically established for the treatment of other cancer types. In general, the movement of radiotracer development (i.e., radiopharmaceutical drug development) in cancer research towards theranostic radioligand approaches has already occurred in nuclear medicine and is attracting other disciplines in the area of (radio)oncology. This approach can generate international consortium project groups focused on unique prospective theranostic clinical trials with the aims of providing cancer patients with the optimal treatment option and obtaining regulatory acceptance by the respective health care systems.

DISCLOSURE

This publication was supported in part by the CAS (RVO: 86652036), project BIOCEV (CZ.1.05/1.1.00/02.0109) from the ERDF, and the GACR to Cyril Bařinka (301/12/1513). Klaus Kopka, Martina Benešová, and Uwe Haberkorn hold property rights to PSMA-617 and PSMA-1007. John Babich is an inventor of MIP-1095, MIP-1072, MIP-1404, and MIP-1405. No other potential conflict of interest relevant to this article was reported.

ACKNOWLEDGMENTS

We thank Sandra Casula, from the German Cancer Research Center, who helped in the editing and careful review of the manuscript. We also thank Springer Nature, the American Chemical Society, and the American Association for Cancer Research for permission to reprint Figures 1, 2, and 8.

REFERENCES

1. Kiess AP, Banerjee SR, Mease RC, et al. Prostate-specific membrane antigen as a target for cancer imaging and therapy. *Q J Nucl Med Mol Imaging.* 2015;59:241–268.
2. Pillai MR, Nanabala R, Joy A, Sasikumar A, Russ Knapp FF. Radiolabeled enzyme inhibitors and binding agents targeting PSMA: effective theranostic tools for imaging and therapy of prostate cancer. *Nucl Med Biol.* 2016;43:692–720.
3. Haberkorn U, Eder M, Kopka K, Babich JW, Eisenhut M. New strategies in prostate cancer: prostate-specific membrane antigen (PSMA) ligands for diagnosis and therapy. *Clin Cancer Res.* 2016;22:9–15.

4. Kratochwil C, Afshar-Oromieh A, Kopka K, Haberkorn U, Giesel FL. Current status of prostate-specific membrane antigen targeting in nuclear medicine: clinical translation of chelator containing prostate-specific membrane antigen ligands into diagnostics and therapy for prostate cancer. *Semin Nucl Med.* 2016;46: 405–418.
5. Hillier SM, Maresca KP, Femia FJ, et al. Preclinical evaluation of novel glutamate-urea-lysine analogues that target prostate-specific membrane antigen as molecular imaging pharmaceuticals for prostate cancer. *Cancer Res.* 2009;69: 6932–6940.
6. Maresca KP, Hillier SM, Femia FJ, et al. A series of halogenated heterodimeric inhibitors of prostate specific membrane antigen (PSMA) as radiolabeled probes for targeting prostate cancer. *J Med Chem.* 2009;52:347–357.
7. Afshar-Oromieh A, Malcher A, Eder M, et al. PET imaging with a [^{68}Ga]gallium-labelled PSMA ligand for the diagnosis of prostate cancer: biodistribution in humans and first evaluation of tumour lesions. *Eur J Nucl Med Mol Imaging.* 2013;40:486–495.
8. Afshar-Oromieh A, Haberkorn U, Eder M, Eisenhut M, Zechmann CM. [^{68}Ga] gallium-labelled PSMA ligand as superior PET tracer for the diagnosis of prostate cancer: comparison with ^{18}F-FECH. *Eur J Nucl Med Mol Imaging.* 2012;39: 1085–1086.
9. Kozikowski AP, Nan F, Conti P, et al. Design of remarkably simple, yet potent urea-based inhibitors of glutamate carboxypeptidase II (NAALADase). *J Med Chem.* 2001;44:298–301.
10. Kozikowski AP, Zhang J, Nan F, et al. Synthesis of urea-based inhibitors as active site probes of glutamate carboxypeptidase II: efficacy as analgesic agents. *J Med Chem.* 2004;47:1729–1738.
11. Jackson PF, Cole DC, Slusher BS, et al. Design, synthesis, and biological activity of a potent inhibitor of the neuropeptidase *N*-acetylated alpha-linked acidic dipeptidase. *J Med Chem.* 1996;39:619–622.
12. Jackson PF, Slusher BS. Design of NAALADase inhibitors: a novel neuroprotective strategy. *Curr Med Chem.* 2001;8:949–957.
13. Foss CA, Mease RC, Fan H, et al. Radiolabeled small-molecule ligands for prostate-specific membrane antigen: in vivo imaging in experimental models of prostate cancer. *Clin Cancer Res.* 2005;11:4022–4028.
14. Pinto JT, Suffoletto BP, Berzin TM, et al. Prostate-specific membrane antigen: a novel folate hydrolase in human prostatic carcinoma cells. *Clin Cancer Res.* 1996;2:1445–1451.
15. Silver DA, Pellicer I, Fair WR, Heston WD, Cordon-Cardo C. Prostate-specific membrane antigen expression in normal and malignant human tissues. *Clin Cancer Res.* 1997;3:81–85.
16. Perner S, Hofer MD, Kim R, et al. Prostate-specific membrane antigen expression as a predictor of prostate cancer progression. *Hum Pathol.* 2007;38:696–701.
17. Eder M, Schäfer M, Bauder-Wüst U, et al. ^{68}Ga-complex lipophilicity and the targeting property of a urea-based PSMA inhibitor for PET imaging. *Bioconjug Chem.* 2012;23:688–697.
18. Zechmann CM, Afshar-Oromieh A, Armor T, et al. Radiation dosimetry and first therapy results with a ^{124}I/^{131}I-labeled small molecule (MIP-1095) targeting PSMA for prostate cancer therapy. *Eur J Nucl Med Mol Imaging.* 2014;41:1280–1292.
19. Barrett JA, Coleman RE, Goldsmith SJ, et al. First-in-man evaluation of 2 high-affinity PSMA-avid small molecules for imaging prostate cancer. *J Nucl Med.* 2013;54:380–387.
20. Benešová M, Bauder-Wüst U, Schäfer M, et al. Linker modification strategies to control the prostate-specific membrane antigen (PSMA)-targeting and pharmacokinetic properties of DOTA-conjugated PSMA inhibitors. *J Med Chem.* 2016;59:1761–1775.
21. Benešová M, Schäfer M, Bauder-Wüst U, et al. Preclinical evaluation of a tailor-made DOTA-conjugated PSMA inhibitor with optimized linker moiety for imaging and endoradiotherapy of prostate cancer. *J Nucl Med.* 2015;56:914–920.
22. Weineisen M, Schottelius M, Simecek J, et al. ^{68}Ga- and ^{177}Lu-labeled PSMA I&T: optimization of a PSMA-targeted theranostic concept and first proof-of-concept human studies. *J Nucl Med.* 2015;56:1169–1176.
23. Rauscher I, Maurer T, Souvatzoglou M, et al. Intrapatient comparison of ^{111}In-PSMA I&T SPECT/CT and hybrid ^{68}Ga-HBED-CC PSMA PET in patients with early recurrent prostate cancer. *Clin Nucl Med.* 2016;41:e397–e402.
24. Rahbar K, Ahmadzadehfar H, Kratochwil C, et al. German multicenter study investigating ^{177}Lu-PSMA-617 radioligand therapy in advanced prostate cancer patients. *J Nucl Med.* 2017;58:85–90.
25. Kratochwil C, Bruchertseifer F, Giesel FL, et al. ^{225}Ac-PSMA-617 for PSMA-targeted α-radiation therapy of metastatic castration-resistant prostate cancer. *J Nucl Med.* 2016;57:1941–1944.
26. Delker A, Fendler WP, Kratochwil C, et al. Dosimetry for ^{177}Lu-DKFZ-PSMA-617: a new radiopharmaceutical for the treatment of metastatic prostate cancer. *Eur J Nucl Med Mol Imaging.* 2016;43:42–51.
27. Yadav MP, Ballal S, Tripathi M, et al. ^{177}Lu-DKFZ-PSMA-617 therapy in metastatic castration resistant prostate cancer: safety, efficacy, and quality of life assessment. *Eur J Nucl Med Mol Imaging.* 2017;44:81–91.
28. Cardinale J, Schäfer M, Benešová M, et al. Preclinical evaluation of ^{18}F-PSMA-1007: a new PSMA ligand for prostate cancer imaging. *J Nucl Med.* 2017;58:425–431.
29. Giesel FL, Hadaschik B, Cardinale J, et al. F-18 labelled PSMA-1007: biodistribution, radiation dosimetry and histopathological validation of tumor lesions in prostate cancer patients. *Eur J Nucl Med Mol Imaging.* 2017;44:678–688.
30. Giesel FL, Kesch C, Yun M, et al. ^{18}F-PSMA-1007 PET/CT detects micrometastases in a patient with biochemically recurrent prostate cancer. *Clin Genitourin Cancer.* December 29, 2016 [Epub ahead of print].
31. Mease RC, Dusich CL, Foss CA, et al. *N*-[*N*-[(*S*)-1,3-dicarboxypropyl]carbamoyl]-4-[^{18}F]fluorobenzyl-L-cysteine, [^{18}F]DCFBC: a new imaging probe for prostate cancer. *Clin Cancer Res.* 2008;14:3036–3043.
32. Rowe SP, Gage KL, Faraj SF, et al. ^{18}F-DCFBC PET/CT for PSMA-based detection and characterization of primary prostate cancer. *J Nucl Med.* 2015;56:1003–1010.
33. Rowe SP, Macura KJ, Ciarallo A, et al. Comparison of prostate-specific membrane antigen–based ^{18}F-DCFBC PET/CT to conventional imaging modalities for detection of hormone-naïve and castration-resistant metastatic prostate cancer. *J Nucl Med.* 2016;57:46–53.
34. Chen Y, Pullambhatla M, Foss CA, et al. 2-(3-{1-Carboxy-5-[(6-[^{18}F]fluoro-pyridine-3-carbonyl)-amino]-pentyl}-ureido)-pentanedioic acid, [^{18}F]DCFPyL, a PSMA-based PET imaging agent for prostate cancer. *Clin Cancer Res.* 2011;17:7645–7653.
35. Rowe SP, Macura KJ, Mena E, et al. PSMA-based [^{18}F]DCFPyL PET/CT is superior to conventional imaging for lesion detection in patients with metastatic prostate cancer. *Mol Imaging Biol.* 2016;18:411–419.
36. Vallabhajosula S, Nikolopoulou A, Babich JW, et al. ^{99m}Tc-labeled small-molecule inhibitors of prostate-specific membrane antigen: pharmacokinetics and biodistribution studies in healthy subjects and patients with metastatic prostate cancer. *J Nucl Med.* 2014;55:1791–1798.
37. Osborne J, Akhtar NH, Vallabhajosula S, et al. Tc-99m labeled small-molecule inhibitors of prostate-specific membrane antigen (PSMA): new molecular imaging probes to detect metastatic prostate adenocarcinoma (PC) [abstract]. *J Clin Oncol.* 2012;30(suppl 5):173.
38. Robu S, Schottelius M, Eiber M, et al. Preclinical evaluation and first patient application of ^{99m}Tc-PSMA-I&S for SPECT imaging and radioguided surgery in prostate cancer. *J Nucl Med.* 2017;58:235–242.
39. Umbricht CA, Benešová M, Schmid RM, et al. ^{44}Sc-PSMA-617 for radiotheragnostics in tandem with ^{177}Lu-PSMA-617: preclinical investigations in comparison with ^{68}Ga-PSMA-11 and ^{68}Ga-PSMA-617. *EJNMMI Res.* 2017;7:9.
40. Afshar-Oromieh A, Hetzheim H, Kratochwil C, et al. The theranostic PSMA ligand PSMA-617 in the diagnosis of prostate cancer by PET/CT: biodistribution in humans, radiation dosimetry, and first evaluation of tumor lesions. *J Nucl Med.* 2015;56:1697–1705.
41. Davis MI, Bennett MJ, Thomas LM, Bjorkman PJ. Crystal structure of prostate-specific membrane antigen, a tumor marker and peptidase. *Proc Natl Acad Sci USA.* 2005;102:5981–5986.
42. Mesters JR, Barinka C, Li W, et al. Structure of glutamate carboxypeptidase II, a drug target in neuronal damage and prostate cancer. *EMBO J.* 2006;25:1375–1384.
43. Pavlícek J, Ptácek J, Barinka C. Glutamate carboxypeptidase II: an overview of structural studies and their importance for structure-based drug design and deciphering the reaction mechanism of the enzyme. *Curr Med Chem.* 2012;19:1300–1309.
44. Pavlicek J, Ptacek J, Cerny J, et al. Structural characterization of P1′-diversified urea-based inhibitors of glutamate carboxypeptidase II. *Bioorg Med Chem Lett.* 2014;24:2340–2345.
45. Wang H, Byun Y, Barinka C, et al. Bioisosterism of urea-based GCPII inhibitors: synthesis and structure-activity relationship studies. *Bioorg Med Chem Lett.* 2010;20:392–397.
46. Plechanovová A, Byun Y, Alquicer G, et al. Novel substrate-based inhibitors of human glutamate carboxypeptidase II with enhanced lipophilicity. *J Med Chem.* 2011;54:7535–7546.
47. Ganguly T, Dannoon S, Hopkins MR, et al. A high-affinity [^{18}F]-labeled phosphoramidate peptidomimetic PSMA-targeted inhibitor for PET imaging of prostate cancer. *Nucl Med Biol.* 2015;42:780–787.
48. Barinka C, Byun Y, Dusich CL, et al. Interactions between human glutamate carboxypeptidase II and urea-based inhibitors: structural characterization. *J Med Chem.* 2008;51:7737–7743.
49. Barinka C, Rovenská M, Mlcochová P, et al. Structural insight into the pharmacophore pocket of human glutamate carboxypeptidase II. *J Med Chem.* 2007; 50:3267–3273.

50. Novakova Z, Cerny J, Choy CJ, et al. Design of composite inhibitors targeting glutamate carboxypeptidase II: the importance of effector functionalities. *FEBS J.* 2016;283:130–143.
51. Dannoon S, Ganguly T, Cahaya H, et al. Structure-activity relationship of ^{18}F-labeled phosphoramidate peptidomimetic prostate-specific membrane antigen (PSMA)-targeted inhibitor analogues for PET imaging of prostate cancer. *J Med Chem.* 2016;59:5684–5694.
52. Zhang AX, Murelli RP, Barinka C, et al. A remote arene-binding site on prostate specific membrane antigen revealed by antibody-recruiting small molecules. *J Am Chem Soc.* 2010;132:12711–12716.
53. Tykvart J, Schimer J, Jancarik A, et al. Design of highly potent urea-based, exosite-binding inhibitors selective for glutamate carboxypeptidase II. *J Med Chem.* 2015;58:4357–4363.
54. Tykvart J, Schimer J, Barinkova J, et al. Rational design of urea-based glutamate carboxypeptidase II (GCPII) inhibitors as versatile tools for specific drug targeting and delivery. *Bioorg Med Chem.* 2014;22:4099–4108.
55. Youn S, Kim KI, Ptacek J, et al. Carborane-containing urea-based inhibitors of glutamate carboxypeptidase II: synthesis and structural characterization. *Bioorg Med Chem Lett.* 2015;25:5232–5236.
56. Horoszewicz JS, Leong SS, Kawinski E, et al. LNCaP model of human prostatic carcinoma. *Cancer Res.* 1983;43:1809–1818.
57. Reubi JC, Waser B, Schaer JC, Laissue JA. Somatostatin receptor sst1-sst5 expression in normal and neoplastic human tissues using receptor autoradiography with subtype-selective ligands. *Eur J Nucl Med.* 2001;28:836–846.
58. Pool SE, Krenning EP, Koning GA, et al. Preclinical and clinical studies of peptide receptor radionuclide therapy. *Semin Nucl Med.* 2010;40:209–218.
59. Aloj L, Aurilio M, Rinaldi V, et al. Comparison of the binding and internalization properties of 12 DOTA-coupled and ^{111}In-labelled CCK2/gastrin receptor binding peptides: a collaborative project under COST Action BM0607. *Eur J Nucl Med Mol Imaging.* 2011;38:1417–1425.
60. Roosenburg S, Laverman P, Joosten L, et al. PET and SPECT imaging of a radiolabeled minigastrin analogue conjugated with DOTA, NOTA, and NODAGA and labeled with ^{64}Cu, ^{68}Ga, and ^{111}In. *Mol Pharm.* 2014;11:3930–3937.
61. Minamimoto R, Hancock S, Schneider B, et al. Pilot comparison of ^{68}Ga-RM2 PET and ^{68}Ga-PSMA-11 PET in patients with biochemically recurrent prostate cancer. *J Nucl Med.* 2016;57:557–562.
62. Zhang J, Li D, Lang L, et al. ^{68}Ga-NOTA-Aca-BBN(7–14) PET/CT in healthy volunteers and glioma patients. *J Nucl Med.* 2016;57:9–14.
63. Luo Y, Pan Q, Yao S, et al. Glucagon-like peptide-1 receptor PET/CT with ^{68}Ga-NOTA-exendin-4 for detecting localized insulinoma: a prospective cohort study. *J Nucl Med.* 2016;57:715–720.
64. Vag T, Gerngross C, Herhaus P, et al. First experience with chemokine receptor CXCR4–targeted PET imaging of patients with solid cancers. *J Nucl Med.* 2016;57:741–746.
65. Herrmann K, Schottelius M, Lapa C, et al. First-in-human experience of CXCR4-directed endoradiotherapy with ^{177}Lu- and ^{90}Y-labeled pentixather in advanced-stage multiple myeloma with extensive intra- and extramedullary disease. *J Nucl Med.* 2016;57:248–251.
66. Bluemel C, Hahner S, Heinze B, et al. Investigating the chemokine receptor 4 as potential theranostic target in adrenocortical cancer patients. *Clin Nucl Med.* 2017;42:e29–e34.
67. Kratochwil C, Giesel FL, López-Benítez R, et al. Intraindividual comparison of selective arterial versus venous ^{68}Ga-DOTATOC PET/CT in patients with gastroenteropancreatic neuroendocrine tumors. *Clin Cancer Res.* 2010;16:2899–2905.
68. Virgolini I, Ambrosini V, Bomanji JB, et al. Procedure guidelines for PET/CT tumour imaging with ^{68}Ga-DOTA-conjugated peptides: ^{68}Ga-DOTA-TOC, ^{68}Ga-DOTA-NOC, ^{68}Ga-DOTA-TATE. *Eur J Nucl Med Mol Imaging.* 2010;37:2004–2010.
69. Breeman WA, de Blois E, Sze Chan H, et al. ^{68}Ga-labeled DOTA-peptides and ^{68}Ga-labeled radiopharmaceuticals for positron emission tomography: current status of research, clinical applications, and future perspectives. *Semin Nucl Med.* 2011;41:314–321.
70. Kratochwil C, Giesel FL, Bruchertseifer F, et al. ^{213}Bi-DOTATOC receptor-targeted alpha-radionuclide therapy induces remission in neuroendocrine tumours refractory to beta radiation: a first-in-human experience. *Eur J Nucl Med Mol Imaging.* 2014;41:2106–2119.
71. Breeman WA, De Jong M, Visser TJ, Erion JL, Krenning EP. Optimising conditions for radiolabelling of DOTA-peptides with ^{90}Y, ^{111}In and ^{177}Lu at high specific activities. *Eur J Nucl Med Mol Imaging.* 2003;30:917–920.
72. Ginj M, Zhang H, Waser B, et al. Radiolabeled somatostatin receptor antagonists are preferable to agonists for in vivo peptide receptor targeting of tumors. *Proc Natl Acad Sci USA.* 2006;103:16436–16441.
73. Wild D, Fani M, Fischer R, et al. Comparison of somatostatin receptor agonist and antagonist for peptide receptor radionuclide therapy: a pilot study. *J Nucl Med.* 2014;55:1248–1252.
74. Fani M, Peitl PK, Velikyan I. Current status of radiopharmaceuticals for the theranostics of neuroendocrine neoplasms. *Pharmaceuticals (Basel).* 2017;10:30.
75. Murphy GP, Su S, Jarisch J, Kenny GM. Serum levels of PSMA. *Prostate.* 2000;42:318–319.
76. Smith-Jones PM, Vallabahajosula S, Goldsmith SJ, et al. In vitro characterization of radiolabeled monoclonal antibodies specific for the extracellular domain of prostate-specific membrane antigen. *Cancer Res.* 2000;60:5237–5243.
77. Bostwick DG, Pacelli A, Blute M, et al. Prostate specific membrane antigen expression in prostatic intraepithelial neoplasia and adenocarcinoma: a study of 184 cases. *Cancer.* 1998;82:2256–2261.
78. Pangalos MN, Neefs JM, Somers M, et al. Isolation and expression of novel human glutamate carboxypeptidases with *N*-acetylated alpha-linked acidic dipeptidase and dipeptidyl peptidase IV activity. *J Biol Chem.* 1999;274:8470–8483.
79. O'Keefe DS, Bacich DJ, Heston WDW. Comparative analysis of prostate-specific membrane antigen (PSMA) versus a prostate-specific membrane antigen-like gene. *Prostate.* 2004;58:200–210.
80. Troyer JK, Beckett ML, Wright GL. Detection and characterization of the prostate-specific membrane antigen (PSMA) in tissue extracts and body fluids. *Int J Cancer.* 1995;62:552–558.
81. Sokoloff RL, Norton KC, Gasior CL, Marker KM, Grauer LS. A dual-monoclonal sandwich assay for prostate-specific membrane antigen: levels in tissues, seminal fluid and urine. *Prostate.* 2000;43:150–157.
82. Luthi-Carter R, Barczak AK, Speno H, Coyle JT. Molecular characterization of human brain *N*-acetylated α-linked acidic dipeptidase (NAALADase). *J Pharmacol Exp Ther.* 1998;286:1020–1025.
83. Evans JC, Malhotra M, Cryan JF, O'Driscoll CM. The therapeutic and diagnostic potential of the prostate specific membrane antigen/glutamate carboxypeptidase II (PSMA/GCPII) in cancer and neurological disease. *Br J Pharmacol.* 2016;173:3041–3079.
84. Wright GL Jr., Grob BM, Haley C, et al. Upregulation of prostate-specific membrane antigen after androgen-deprivation therapy. *Urology.* 1996;48:326–334.
85. Sweat SD, Pacelli A, Murphy GP, Bostwick DG. Prostate-specific membrane antigen expression is greatest in prostate adenocarcinoma and lymph node metastases. *Urology.* 1998;52:637–640.
86. Mannweiler S, Amersdorfer P, Trajanoski S, Terrett JA, King D, Mehes G. Heterogeneity of prostate-specific membrane antigen (PSMA) expression in prostate carcinoma with distant metastasis. *Pathol Oncol Res.* 2009;15:167–172.
87. Maddalena ME, Fox J, Chen J, et al. ^{177}Lu-AMBA biodistribution, radiotherapeutic efficacy, imaging, and autoradiography in prostate cancer models with low GRP-R expression. *J Nucl Med.* 2009;50:2017–2024.
88. Gerlinger M, Rowan AJ, Horswell A, et al. Intratumor heterogeneity and branched evolution revealed by multiregion sequencing. *N Engl J Med.* 2012;366:883–892.
89. Yap TA, Gerlinger M, Futreal PA, Pusztai L, Swanton C. Intratumoral heterogeneity: seeing the wood for the trees. *Sci Transl Med.* 2012;4:127ps10.
90. Mitchell T, Neal DE. The genomic evolution of human prostate cancer. *Br J Cancer.* 2015;113:193–198.
91. Murphy TM, Severns V, Brown DC, et al. Prostate cancer targeting motifs: expression of $\alpha_v\beta_3$, neurotensin receptor 1, prostate specific membrane antigen, and prostate stem cell antigen in human prostate cancer cell lines and xenografts. *Prostate.* 2011;71:1–17.
92. Ananias HJ, van der Heuvel MC, Helfrich W, de Jong IJ. Expression of the gastrin-releasing peptide receptor, the prostate stem cell antigen and the prostate-specific membrane antigen in lymph node and bone metastases of prostate cancer. *Prostate.* 2009;69:1101–1108.
93. Afshar-Oromieh A, Hetzheim H, Kübler W, et al. Radiation dosimetry of ^{68}Ga-PSMA-11 (HBED-CC) and preliminary evaluation of optimal imaging timing. *Eur J Nucl Med Mol Imaging.* 2016;43:1611–1620.
94. Kratochwil C, Giesel FL, Stefanova M, et al. PSMA-targeted radionuclide therapy of metastatic castration-resistant prostate cancer with ^{177}Lu-labeled PSMA-617. *J Nucl Med.* 2016;57:1170–1176.
95. Herrmann K, Bluemel C, Weineisen M, et al. Biodistribution and radiation dosimetry for a probe targeting prostate-specific membrane antigen for imaging and therapy. *J Nucl Med.* 2015;56:855–861.
96. Szabo Z, Mena E, Rowe SP, et al. Initial evaluation of [^{18}F]DCFPyL for prostate-specific membrane antigen (PSMA)-targeted PET imaging of prostate cancer. *Mol Imaging Biol.* 2015;17:565–574.
97. Cho SY, Gage KL, Mease RC, et al. Biodistribution, tumor detection, and radiation dosimetry of ^{18}F-DCFBC, a low-molecular-weight inhibitor of prostate-specific membrane antigen, in patients with metastatic prostate cancer. *J Nucl Med.* 2012;53:1883–1891.